Model parameterization and experimental design issues in nearshore bathymetry inversion

C. Narayanan

Marine Modeling and Analysis Branch, National Weather Service, Camp Springs, Maryland, USA

V. N. Rama Rao

Earth Resources Laboratory, Massachusetts Institute of Technology, Cambridge, Massachusetts, USA

J. M. Kaihatu

Oceanography Division, Naval Research Laboratory, Stennis Space Center, Mississippi, USA

[1]   We present a general method for approaching inverse problems for bathymetric determination under shoaling waves. We run the Korteweg-de Vries (KdV) model for various bathymetric representations while collecting data in the form of free-surface imagery and time series. The sensitivity matrix provides information on the range of influence of data on the parameter space. By minimizing the parameter variances, three metrics based on the sensitivity matrix are derived that can be systematically used to make choices of experiment design and model parameterization. This analysis provides insights that are useful, irrespective of the minimization scheme chosen for inversion. We identify the characteristics of the data (time series versus snapshots, early time measurements versus long-duration measurements, nearshore measurements versus offshore measurements), and model (bathymetry parameterizations) for inversion to be possible. We show that Bruun/Dean and Exponential bathymetric parameterizations are preferred over polynomial parameterizations. The former can be used for inversion with both time series and snapshot data, while the latter is preferably used only with snapshot data. Also, guidelines for time separation between snapshots and spatial separation between time series measurements are derived.   *INDEX TERMS:* 4560 Oceanography: Physical: Surface waves and tides (1255); 4546 Oceanography: Physical: Nearshore processes; 4594 Oceanography: Physical: Instruments and techniques; 4255 Oceanography: General: Numerical modeling; *KEYWORDS:* experimental design, model parameterization, bathymetric inversion

1.   Introduction

[2]   Accurate knowledge of nearshore bathymetry and its evolution in time is critical to the understanding of coastal processes and its impact on shoreline evolution. Given a priori knowledge of environmental properties such as bathymetry, sophisticated numerical models can be run to simulate these coastal processes (the so-called "forward modeling" approach). However, direct measurement of the bathymetry is generally difficult and expensive. Hence, inverse techniques have been postulated to determine the bathymetry from properties of the ocean free surface. (The term "inverse techniques" is typically associated with any methodology that gleans knowledge of physical processes from observations. In our application of the term in this paper, however, we limit its use to describing procedures akin to data assimilation.)

[3]   The current state of the forward modeling of ocean wave propagation, breaking, and the resultant effects on nearshore hydrodynamics is quite advanced. For example, *Chen et al.* [1999, 2000] and *Kennedy et al.* [2000] have demonstrated the ability to predict a wide variety of nearshore processes with good accuracy using a phase-resolving time domain Boussinesq wave model [*Wei et al.*, 1996]. These models can determine the free surface profiles and wave-induced currents for varying bathymetries if the initial conditions and boundary conditions are known, essentially providing a comprehensive picture of the nearshore environment from a single model. It would appear logical, then, that these physically complete models could be used to provide the physical realism needed to develop successful inverse techniques.

[4] As intimated above, inverse methods include data assimilation. Assimilative techniques have been used in meteorology and oceanography for some time [e.g., *Ghil*, 1989; *Bennett*, 1992; *Moore*, 1991]. They have been used to improve initial/boundary conditions [e.g., *Yu and O'Brien*, 1992] and to estimate best-fit parameters for modeling [e.g., *Thacker and Long*, 1988; *Navon*, 1997]. However, their use in the solution of nearshore wave transformation problems is quite recent; *Feddersen et al.* [2004] and *Özkan-Haller and Long* [2002] have used adjoint methods to estimate the friction coefficients for a nearshore circulation model.

[5] There has been some prior work on bathymetric estimation; these can be broadly classified into two categories. Some depth inversion methods rely upon an a priori specified dispersion relationship relating the wave frequency, wavelength, and water depth. These wave properties are computed from data (usually remotely sensed). We refer to these methods as "a priori" methods, since they use an assumed relationship between wave properties and water depth. Other depth inversion methods, in contrast, use numerical models for wave propagation to provide the physics to the inversion process; these methods have no a priori knowledge or assumptions concerning the physics of wave propagation, other than that the forward model used contains the appropriate physics. We refer to this second set of methods as "full" inversion methods, since (potentially) all physical properties represented in the model used can either be used as input data or can be determined from the inversion process, with no assumed relationship.

[6] In the a priori inversion approach [e.g., *Stockdon and Holman*, 2000; *Holland*, 2001; *Dugan et al.*, 1996; *Bell*, 1999], spatially distributed, time registered estimates of wave phase from remotely sensed measurements are used with an assumed dispersion relationship to obtain the water depth. The disadvantage with this approach is that it does not capture amplitude dispersion effects adequately in regions of moderate to high wave nonlinearity, especially near breaking. Model-based a priori approaches have been posited by *Grilli* [1998], *Kennedy et al.* [2000], and *Misra et al.* [2000]. *Grilli* [1998] used a fully nonlinear one-dimensional wave transformation model to codify the effect of nonlinearity on the observable properties of the wave field, then developed (via an empirical relation) two algorithms for determining the water depth. *Kennedy et al.* [2000] and *Misra et al.* [2000] used the fully nonlinear Boussinesq model of *Wei et al.* [1996] to reconstruct the bathymetry. *Kennedy et al.* [2000] used two snapshots of water surface elevations as data, calculated the phase speed at both times and, based on the phase speed mismatch between the model and data, updated the depth. The overall depth was predicted quite accurately. In an effort to avoid using the Boussinesq model inside an iterative loop, however, they make use of a priori information concerning the connection between waves properties and water depth to guide their corrections to their water depth estimates. The correction was itself empirically derived, thus ostensibly limiting its scope.

[7] In the full inversion approach, there are no assumptions for the relationship between the wave characteristics and water depth; it is defined implicitly by the governing equation representing the wave propagation. Once the appropriate equation is chosen and measurements collected,

a minimization scheme is used, where bathymetry is varied until the misfit between the observed wave characteristics and those predicted by the model is minimal. The full inversion has the advantage of accounting for all observed surface wave characteristics, the specifics of which depend on the type of data used. *Narayanan and Kaihatu* [2000] and *Kaihatu and Narayanan* [2001] detailed a full inversion technique, using a time-dependent Korteweg-de Vries (KdV) model to provide the wave physics and the Levenberg-Marquardt numerical optimization method [e.g., *Press et al.*, 1986] to perform the inversion and estimate the water depth. The depth profiles were represented by equilibrium beach profiles, which are analytic functions dependent on parameters [see, e.g., *Dean and Dalrymple*, 2001]. These parameters, while ostensibly functions of wave climate, sediment size, etc., are usually used in a best-fit sense in practical situations. The use of equilibrium beach profiles by *Narayanan and Kaihatu* [2000] and *Kaihatu and Narayanan* [2001] reduced the depth inversion problem to a parameter estimation problem. However, they also noted that non-uniqueness and parameter identifiability problems were clearly present, even in a greatly reduced search. It has been determined in other disciplines that complex forward models are often associated with parameter identifiability difficulties [*Beck*, 1987] when used as part of inverse schemes. While the choice of numerical technique for optimization may be a factor, the nature of the measured data and parameters to be estimated are as important to the success of the inversion procedure. In this work, we will restrict ourselves to the full inversion approach.

[8] One consideration in ascertaining the probable success of an inversion procedure is determining whether the measured variable is sufficiently sensitive to variations of the parameters sought. For example, if there are areas in the domain where the characteristics of the free surface do not change appreciably as the depth changes, then estimation of the water depth from the free surface characteristics may be non-unique in those areas. This evaluation can be performed prior to inversion. Various forms of sensitivity-based analysis have been used quite successfully to improve inversion robustness in a variety of disciplines [*Rao*, 1996; *Xia et al.*, 1999; *Sun et al.*, 2001; *Brun et al.*, 2001].

[9] We extend these approaches by framing sensitivity-based analysis as a consequence of minimizing parameter variance. We develop three metrics based on sensitivity analysis that can be systematically used to make choices of experiment design and model parameterization that reduce parameter variance. This analysis provides insights that are physically (and practically) useful, irrespective of the minimization scheme chosen for inversion. We identify the characteristics of the data and model for inversion to be possible. Specifically, we address the following issues in the paper: (1) locations of data collection in the domain for optimal inversion, and the dependence of these locations on the nature of the data; (2) extent of domain over which bathymetry can be reliably estimated; (3) establishment of rational criterion by which representations of the bathymetry (bathymetric parameterizations) can be ranked; and (4) convergence characteristics of different parameters within a selected representation of the depth.

[10] We formulate the forward problem in section 2 and the inversion framework in section 3. The approach for

sensitivity analysis is described in section 4. Section 5 provides results and discussion, and section 6 concludes the study.

2. Wave Propagation Models and Bathymetry Representations

[11] Because we are not employing any specific a priori assumptions in our inversion process, the selection of the appropriate model for representing the physical processes of wave transformation is very crucial. As mentioned previously, there are several sophisticated models available for representing the full kinematic and dynamic character of transforming waves (that of *Wei et al.* [1996] as a particular example). In a general situation, waves transform over two-dimensional bathymetry and break; the nonlinearity of the wave at near breaking becomes considerable, well out of the range of weakly nonlinear models.

[12] However, if the viewpoint is switched toward emphasizing the inversion itself (and associated analysis), and we remain within the validity of our forward model (at least at this preliminary stage), then the choice of model becomes less critical. In the spirit of prior works on the development of data assimilative systems [e.g., *de las Heras and Janssen*, 1992], our ''data'' will consist of output from our forward model, generated using our target bathymetry; this completely obviates the question of the validity of the model since both data and model are entirely consistent. (It is likely that the use of actual measurements will require as sophisticated a forward model as is practical to operate.) Thus, in order to maintain simplicity in the development of the inversion system, we will utilize the same KdV wave propagation model used by *Narayanan and Kaihatu* [2000] and *Kaihatu and Narayanan* [2001]; the appropriate reasoning and caveats will be discussed in a later section.

[13] In addition, to simplify the initial development of the inversion system, we incorporate data (understood to be model output for this developmental stage) comprised of the same physical property as that offered by the model. In this case, we assume that measurements of the free surface evolution $\eta(x, t)$ comprise our data. They may be obtained either as a free-surface imagery (i.e., snapshots at different times) $\eta(\mathbf{x}, t = t_0)$, or in the form of time series at fixed locations, $\eta(\mathbf{x} = x_0, t)$. The KdV equation relates the bathymetry or water depth, $h(\mathbf{x})$, to the free-surface elevations, $\eta(\mathbf{x}, t)$. We defer the practicality and reasoning behind this selection to a later section.

2.1. Wave Model

[14] As mentioned previously, our forward model is the KdV model. This equation describes one-dimensional shallow water waves with small but finite amplitudes and is the simplest equation that combines nonlinearity and frequency dispersion. The KdV equation can predict the wave height and wave profile skewness quite well as a wave shoals (C. Narayan, Comparison of different KdV equations with respect to wave shoaling, submitted to *Ocean Modelling*, 2004) and can be expressed as

$$\eta_t + (c_0\eta)_x + \left[\frac{3c_0\eta^2}{4h} - \frac{h^2\eta_{xt}}{6}\right]_x = 0, \tag{1}$$

Table 1. Best-Fit Parameters to the Duck, North Carolina, Profile

Parameterization	Values
Bruun/Dean	$B = 0.660$, $\beta = 0.400$
Exponential	$E = 0.147$, $\epsilon = 0.500$
Polynomial	$p_0 = -0.678$, $p_1 = 0.540$, $p_2 = -0.815$, $p_3 = 0.836$,

where $\eta(x, t)$ is the free surface elevation of the water surface, h is water depth, $c_0(=\sqrt{gh})$ is the local phase speed, g is gravitational acceleration, x is the cross-shore spatial coordinate, and t is time. Subscripts x and t denote partial derivatives. It is noted that this model is only adequate for weakly nonlinear, weakly dispersive waves, and as such cannot describe the highly nonlinear wave characteristics near breaking, nor is it capable of accurately propagating waves (nonlinear or otherwise) in deep water. Additionally, wave dissipation due to breaking is not included, and wave reflection cannot be modeled. While this does seem inappropriate, we wish to re-emphasize that this model will be used both for generating our requisite data and for the forward model; thus the included physics of the model match those of the input data.

[15] For a model such as the KdV equation, we require both an initial condition of the form $\eta(x, 0)$ and a boundary condition $\eta(0, t)$. This has been extensively discussed by *Bona and Bryant* [1973].

[16] The model is initialized by a wave maker ($\eta(0, t)$) at the offshore end of the domain. The waves leave the domain smoothly at the coast. The KdV equation is modeled using a second-order, three-level finite difference scheme developed by *Eilbeck and McGuire* [1975]. A fourth-order *Shapiro* [1970] filter is used to damp the high-frequency waves. Further, a sponge layer of 1 m is applied to absorb the wave energy at the shore.

2.2. Bathymetry Parameterizations

[17] On the basis of the dissipation rate of spilling breakers and the distance over which the dissipation occurs, *Bruun* [1954] and *Dean* [1977] developed the equilibrium beach profile, a parameterization of the cross-shore bathymetry profile which collapses the description of the water depth into a shape modified by adjustable parameters. Many different profile parameterizations have been advanced since. In general, these parameterizations take the form

$$h = h(\mathbf{m}, x), \tag{2}$$

where $\mathbf{m}$ are the model parameters associated with a specific parameterization. The different parameterizations attempted are described below. Please refer to Table 1 for the different parameters used.

2.2.1. Discrete Depths as Parameters

[18] The simplest bathymetric parameterization involves treating each individual water depth in a bathymetric profile as a distinct, discrete parameter. In this case, the bathymetry can be represented as $h_1, h_2, h_3, \ldots, h_M$ where there are M points in the domain. In this case, the M different parameters that need to be estimated are

$$\mathbf{m} = \{h_1, h_2, h_3, \ldots, h_M\}^T. \tag{3}$$

This representation of the depth is obviously the most faithful. However, problems associated with non-uniqueness

arise with a large number of parameters [*Narayanan and Kaihatu*, 2000].

2.2.2. Bruun/Dean Profile

[19] The best-known and most commonly used beach profile is the Bruun/Dean profile. In the classical parameterization development, energy dissipation arguments were used to derive the supposition that the water depth increased offshore in proportion to $x^{2/3}$ [*Bruun*, 1954; *Dean*, 1977]. However, we choose to frame the exponent as another free parameter to be estimated; thus the water depth is parameterized as

$$h(x) = -Bx^{\beta}. \tag{4}$$

Only two unknown quantities, B and β, need to be estimated. A shortcoming of this equation is that it has infinite slope at the shoreline, though later work [*Larson*, 1995] has eliminated this difficulty. In this paper, we also use an alternate representation of equation (4), which results from normalizing the offshore coordinate x by the domain length L (hereinafter "x-normalized"):,

$$h(x) = -B\left(1 - \frac{x}{L}\right)^{\beta}. \tag{5}$$

It is felt that in several instances, the normalized version of the depth parameterization offers more robustness.

2.2.3. Exponential Profile

[20] *Bodge* [1992] used an exponential profile of the form

$$h(x) = -E[1 - e^{-\epsilon x}], \tag{6}$$

where E and ϵ are the unknown coefficients. *Bodge* [1992] demonstrated that this exponential profile more closely approximates the 504 measured profiles of *Hayden et al.* [1975] than the Bruun/Dean profile. We use an x-normalized version of the exponential profile,

$$h(x) = -E\left[1 - e^{-\epsilon\left(1 - \frac{x}{L}\right)}\right]. \tag{7}$$

2.2.4. Polynomial Profile

[21] The bathymetry can also be represented as a $(M - 1)$th-order polynomial, with M unknowns, of the form

$$h(x) = p_M x^{M-1} + p_{M-1} x^{M-2} + \ldots + p_1, \tag{8}$$

Here, the model parameters are

$$\mathbf{m} = \{p_1, p_2, p_3 \ldots, p_M\}^T. \tag{9}$$

Often a fourth- or fifth-order equation will suffice to adequately represent the bathymetry. *Komar and McDougal* [1994] show that a fifth-order polynomial is able to fit the equilibrium beach profile from the Nile Delta, Egypt. Alternately, an x-normalized version,

$$h(x) = p_M\left(\frac{x}{L}\right)^{M-1} + p_{M-1}\left(\frac{x}{L}\right)^{M-2} + \ldots + p_1, \tag{10}$$

can also be used.

[22] Note that there are many other bathymetric parameterizations possible. However, the focus of this paper is to distinguish between the most commonly used parameterizations.

2.3. Data

[23] Our goal is to describe the bathymetric characteristics given an estimate of the relevant physics (the model) and measurements of the observable manifestations of the physics (data). The nature of the data is thus of relevance. In general, the data can consist of measurements of any observable characteristic of the evolving wave field, whether deterministic (free surface elevation, phase speed) or statistical (directional spectra, significant wave height, peak period, etc.). For the purposes of this discussion, we will assume that data consist of various records of free surface elevations. This comprises an exact connection between the dependent variable in the KdV model and the measured data, and eliminates potential error in the conversion between different wave field properties (e.g., surface velocity to surface elevation) or in the interpretation of imagery in the representation of wave variables (e.g., correlating brightness intensity from video imagery to wave dissipation). We note that there is nothing in our ensuing development that precludes the incorporation of different types of data from various sources.

[24] Direct measurement of the free surface elevation is possible in two forms: temporally sparse, spatially dense snapshots of the free surface, or spatially sparse, temporally dense time series. The latter can be gotten from wave riders or wave gauge measurements, while the former is obtainable from airborne terrain mapping (ATM) lidar measurements. This measurement platform is capable of high spatial resolution (on the order of 1.5 m [*Hwang et al.*, 2001]). Furthermore, forward and backward scans of the instrument can be separated; however, these offer no more than 2 s of additional temporal information.

3. Inverse Problem of Bathymetry Estimation

[25] The inverse problem, as mentioned earlier, consists of estimating bathymetric parameters given realizations of the evolving wave field (in terms of free surface elevations). In this section we discuss our methodology for performing this inversion.

[26] Let the wave surface elevation snapshot data vector be $\bar{\eta}(\mathbf{x}, t = t_0)$, where

$$\bar{\eta}(\mathbf{x}, t = t_0) = \{\bar{\eta}_1, \bar{\eta}_2, \bar{\eta}_3, \ldots, \bar{\eta}_N\}^T \tag{11}$$

are measured at locations $\mathbf{x} = \{x_1, x_2, x_3, \ldots, x_N\}$. We are interested in estimating M parameters. It is assumed that $N > M$, ensuring an overdetermined problem. Let the model be defined as

$$\mathbf{h} = \eta(\mathbf{h}(\mathbf{m}), \mathbf{x}, t). \tag{12}$$

Evaluating the model at the discrete locations $\mathbf{x}$, and at a specific time t_0 for a specified bathymetry h(m), we obtain the surface elevation snapshot at the measurement locations,

as predicted by the forward model. Then the objective function to be minimized, E, can be expressed as

$$E = (\bar{\eta}(\mathbf{x}, t_0) - \eta(\mathbf{x}, t_0))^T (\bar{\eta}(\mathbf{x}, t_0) - \eta(\mathbf{x}, t_0)). \quad (13)$$

The objective function can be defined analogously for time series data. This minimization can be accomplished by global search methods or nonlinear least squares. If using the latter, an initial guess $\mathbf{m}^1$ is made and the following equation is solved iteratively:

$$\mathbf{m}^{i+1} = \mathbf{m}^i + (\mathbf{A}^T\mathbf{A} + \delta)^{-1} \mathbf{A}^T (\bar{\eta} - \eta^i), \quad (14)$$

until successive estimates of the model parameters change minimally. The superscripts refer to the iteration in which the parameters and model are estimated and δ is a diagonal matrix of damping values. The damping can be varied using the Levenberg-Marquardt algorithm. The matrix $\mathbf{A}$ is the Jacobian matrix or the sensitivity matrix, and its columns are the derivative of η with respect to the model parameters.

[27] Given the complexity of typical wave shoaling forward models, and the number of forward model evaluations that will be required to obtain a solution, the full inversion will be computationally intensive. Further, inverse problems with complex forward models often result in meaningless solutions due to parameter identifiability issues [*Beck*, 1987]. The sensitivity-based approach detailed here addresses the latter, so that the full inversion can be performed robustly.

[28] Parameter identifiability in the least squares sense is dependent on the uniqueness and stability of the inverse solution and on the observational data characteristics [*Sun et al.*, 2001; *Chavent*, 1987; *Kitamura and Nakirigi*, 1977, etc.]. If the solution has multiple discrete minima or a continuous range of minima in a given parameter region, we are solving a non-unique problem. The latter is typical of models where two or more parameters are strongly correlated, producing a "valley" in error space along which all combinations of these parameters lead to comparable minimizations. If the least squares solution is continuously dependent on measurement errors, the solution is stable. This ensures that small perturbations due to measurement or computational noise do not produce large variations in the computed inverse solution. Stability and uniqueness are related effects, with some forms of non-uniqueness causing instability. Finally, choices in when and where data are observed govern how sensitive the measurements are to the unknown parameters. Parameters will be poorly identified if the data have little or no sensitivity to the parameters.

4. Sensitivity Analysis

[29] The parameter covariance matrix is defined as

$$\mathbf{V} = \sigma_d^2 (\mathbf{A}^T\mathbf{A})^{-1}, \quad (15)$$

where σ_d^2 is the data variance, equal to $(\bar{\eta} - \eta)^T (\bar{\eta} - \eta)/(N - M)$. The diagonal elements of this matrix specify the variance of the parameters, while the off-diagonals specify the pairwise covariances between the parameters. The determinant of the covariance matrix is a measure of the volume of parameter uncertainty at a given location in

the parameter space and is also termed as the generalized variance. Minimizing this volume amounts to reducing the uncertainty associated with all parameter estimates, and this is our criterion for experiment design and for comparing different bathymetry parameterizations.

$$\min \, det(\mathbf{V}) = \sigma_d^2 \, \min \, det\left((\mathbf{A}^T\mathbf{A})^{-1}\right). \quad (16)$$

However, for a given level of parameter uncertainties or variances along the diagonal, the presence of cross correlations between the parameters reduces the determinant value. Even with parameters of high uncertainty, strong correlations can lead to small determinant values. In fact, in the limit of two or more parameters being equal except for a multiplicative constant, the determinant becomes identically zero. Thus, blind minimization of the determinant does not necessarily lead to parameter estimates of low uncertainty. Hence we decompose the covariance matrix as follows so that the parameter variance and cross correlations can be minimized simultaneously:

$$\min \, det(\mathbf{V}) = \sigma_d^2 \, \max \, det(\mathbf{A}^T\mathbf{A}), \quad (17)$$

$$\propto \max \, det\left(W^{-1}W\mathbf{A}^T\mathbf{A}WW^{-1}\right). \quad (18)$$

W is a diagonal matrix defined as

$$W_{kk} = \left((\mathbf{A}^T\mathbf{A})_{kk}\right)^{-1/2}, \quad (19)$$

with the notation that subscripts in $(\mathbf{A}^T\mathbf{A})_{kk}$ refer to the kth diagonal element. $W\mathbf{A}^T\mathbf{A}W$ has ones along its diagonal and is identical to the correlation matrix. Thus

$$\min \, det(\mathbf{V}) \propto \max \, det(W^{-2}) \, \max \, det(W\mathbf{A}^T\mathbf{A}W), \quad (20)$$

$$\propto \max \, \prod_{k=1}^{M} (\mathbf{A}^T\mathbf{A})_{kk} \, \min \, C(W\mathbf{A}^T\mathbf{A}W), \quad (21)$$

where the first term is the product of the diagonal elements of the $(\mathbf{A}^T\mathbf{A})$, and is maximized when each element is maximized. Minimizing the condition number, defined as the ratio of the largest eigenvalue to the smallest, is equivalent to maximizing the determinant. In the limit of uncorrelated parameters the largest and smallest eigenvalue are 1, and the condition number is also 1. In all other cases, the condition number is greater than 1. In the limit of two or more parameters being equal except for a multiplicative constant, the condition number tends to infinity. Therefore parameter variances are minimized if the sensitivity of the data to the unknown parameter values is maximized while the correlation among the parameters is maintained at its lowest possible level. This is the basis for our experiment design and parameter selection guidelines.

[30] We relate the above two goals in terms of properties of the sensitivity matrix, $\mathbf{A}$.

$$(\mathbf{A}^T\mathbf{A})_{kk} = (2 - \text{norm of } k\text{th column of A})^2, \quad (22)$$

$$C(W\mathbf{A}^T\mathbf{A}W) = (\kappa(\mathbf{A}))^2, \quad (23)$$

Table 2. Sensitivity Metrics and Their Preferred Conditions

Metric	Preferred Conditions
Magnitude of the columns of **A**	at or close to a maximum
2-norm of columns of **A**	at or close to a maximum
Scaled condition number of **A**	Small (1–100)

where κ (**A**) is the scaled condition number of **A** [*Belsley*, 1991]. Hence, with snapshot data, for example, computing the 2-norm of the columns of A, at different times, identifies temporal locations where the M columns attain a maximum, which are the preferred times for snapshots. However, the spatial ranges over which the snapshot is best acquired cannot be deduced from this. The column magnitudes of **A** at a given time provides this information. Thus with space-time data, examining the magnitude and the 2-norm of the columns of **A** helps identify the spatial and temporal ranges where sensitivity is maximized and data are best acquired.

[31] Thus we propose three metrics that can be examined to minimize parameter variance: column magnitude of **A**, 2-norm of the columns of **A**, and scaled condition number of **A**. Preferred ranges of data acquisition are those locations where the first two metrics attain a maximum while the third metric is a minimum (close to 1), for all parameters. Similarly, model parameterizations are ranked based on all three metrics being close to the preferred values (see Table 2). Large sensitivity magnitudes imply parameters that are well constrained by the data, while uncorrelated parameters are necessary for numerically stability. Thus conclusions on experiment design and model parameterization should be drawn by interpreting the three metrics collectively. Cases of large sensitivity with strongly correlated parameters or poor sensitivity with uncorrelated parameters are to be avoided.

[32] Since the goal is to gain insights into experiment design and model parameterization, the sensitivity analysis proposed here is to be performed before data have been acquired. To proceed, approximate representative bathymetry profiles are identified. These can be created based on a priori information on the expected bathymetry profiles in the region where the data are to be acquired.

[33] The first step is to evaluate the derivative of the model or surface elevation (η) with respect to the parameters defining the bathymetry. Given N values of a surface elevation snapshot $\eta(\mathbf{x}, t = t_0)$, and M model parameters $\mathbf{m}$, a $N \times M$ Jacobian or sensitivity matrix **A**, can be defined as

$$A_{jp} = \frac{\partial \eta_j}{\partial m_p}, j = 1, 2, 3, \ldots, N; p = 1, 2, 3, \ldots, M. \quad (24)$$

Since the true parameter values are not known, the sensitivity matrix is evaluated at multiple locations in its expected neighborhood or for a range of representative bathymetries.

[34] Alternatively, $\mathbf{A_s}$ is the normalized sensitivity matrix, or the nondimensional Jacobian matrix and is defined as

$$A_{s(jp)} = \frac{\partial \left(\ln \eta_j \right)}{\partial \left(\ln m_p \right)} = \frac{m_p}{\eta_j} \frac{\partial \eta_j}{\partial m_p}. \quad (25)$$

The three metrics are defined for the normalized sensitivity matrix, but replacing **A** with $\mathbf{A_s}$. In general applications of this technique, analytical derivatives are not possible to evaluate; we use a finite difference approximation to the derivative.

4.1. Column Magnitude of Sensitivity Matrix A

[35] The first metric is the magnitude of the columns (or "column magnitude") of **A** defined as $|A_{jk}|$, where $j = 1, 2, 3, \ldots, N$ for the kth column.

[36] Large values in the kth column of the sensitivity matrix identify the spatial or temporal domain over which the surface elevation is most sensitive to change in the bathymetry parameter m_k. The preferred domain for data acquisition is where this metric is at or close to its maximum. Assuming that data consisted of snapshots, data in the spatial region near the column magnitude maximum exhibit the greatest sensitivity to changes in the parameters sought, and thus have a greater effect on the subsequent parameter estimation than data outside this domain. Second, because one has as many columns as parameters, comparison of column magnitude maxima across the columns offers information on the relative ease of estimation of different parameters. Parameter convergence rates during inversion tend to be proportional to sensitivity magnitudes, since by definition the latter quantifies the change in parameter values for a given perturbation in the data. Parameters with larger sensitivities are likely to converge faster and are associated with smaller variances.

[37] For a given data acquisition domain, comparing the magnitudes of the columns corresponding to different bathymetry parameterizations is a means to rank them. Parameterizations that lead to large sensitivity for all its parameters are preferred. However, when comparing different parameterizations, $\mathbf{A}_s$, whose columns are nondimensional, is used. This allows a rational comparison of data sensitivity to parameters that can have different physical meanings, and potentially different magnitude scales [e.g., *Kokotovich*, 1964; *Kreindler*, 1968; *Sun et al.*, 2001]. When the unknown bathymetry is two-dimensional, sensitivity magnitudes can be analogously defined.

4.2. The 2-Norm of the Columns of A

[38] With snapshot data (say), evaluating this metric at different times will illustrate the preferred times when snapshots are best acquired for inverting for the kth parameter. If using the normalized sensitivity matrix $\mathbf{A}_s$, this metric is defined analogously. Time ranges where the 2-norm of **A** is large (at or close to its maximum) for all the parameters of a given parameterization identify the domain over which snapshot data are most sensitive to all parameters and are most conducive for inversion. As before, the normalized sensitivity matrix is used when comparing different parameterizations. In two-dimensional bathymetry estimation, the column norms can still be interpreted analogously.

4.3. Scaled Condition Number of A

[39] If there is approximate or complete linear dependence in the columns of **A**, it means that a misfit in surface elevation can be compensated approximately or exactly by a change in more than one combination of the parameters. This means that all parameters are not uniquely identifiable, even if their sensitivities are high. If nonlinear least squares inversion is used in the presence of such colinearity, it

would lead to poor convergence or even divergence. If global search methods are used, this underlying correlation between parameters would manifest in the form of jointly uncertain parameters. It must be noted that while correlations are driven by the chosen parameterization, this metric provides information about whether its effects can be mitigated with an appropriate choice of data ranges, or, given two parameterizations, this metric can identify the relative merits of each for a given data range. Often, singular value decomposition or similar methods are employed to obtain orthogonal parameterizations. This metric can be used in conjunction with those approaches with the same interpretation.

[40] The scaled condition number of a matrix is insensitive to matrix scaling, and its magnitude can be interpreted meaningfully. When the columns of a matrix are orthogonal, the scaled condition number is 1, while for any other situation, it is greater than 1. Scaled condition numbers much greater than 100, on the order of 10^4–10^6 are typically associated with strong colinearity-related problems and are ill conditioned [*Belsley*, 1991; *Noble*, 1969]. Large values of condition number also indicate strong sensitivity of the inversion to measurement or numerical noise [*Strang*, 1980]. In this case, the inverted solution is not stable and can be strongly perturbed by even small perturbations in the data due to noise or computational round-off. For snapshot data (say), the sensitivity matrix and its condition number are evaluated at different time instants. Ideal locations for data acquisition and preferred parameterizations are characterized by low values of scaled condition number, preferably close to 1.

5. Results and Discussion

[41] To demonstrate the sensitivity analysis, we use a bathymetric profile measured at the Field Research Facility at Duck, North Carolina, during the DELILAH experiment [*Birkemeier et al.*, 1997]. The morphological characteristics of the area include frequent sandbar formation, which lends the profile a non-monotonic shape. We readily aver that there are no bathymetric parameterizations at our disposal that admit barred profiles, and thus we are unable to obtain bars with our present formulation. However, there is some promising work on adding random bars to equilibrium beach profiles [*Pruszak and Róyski*, 1997], and subsequent parameterizations of barred profiles can easily be accommodated by the technique described herein.

[42] Our domain is shown in Figure 1. It consists of a bathymetric profile from Duck, North Carolina, in which the bar is not pronounced. The length of the domain in the DELILAH experiment is 1125 m over which the depth changes by 12.86 m. Hence the ratio of the length to depth of the domain is 87.5. The computational domain is the scaled version of the DELILAH experiment. The length of the numerical domain is 35 m, reaching an offshore depth $h_0 = 0.4$ m. The wave maker forcing consists of time series of random waves taken from the Texel- Marsden-Arsloe (TMA) spectrum [—it *Hughes*, 1984] with a peak frequency of 0.2/s and with a narrowness coefficient $\gamma = 3.3$, redolent of a fairly broad spectrum. The maximum wave height at the wave maker (H) is 0.065 m. Therefore two representative nondimensional numbers, the relative wave height ($\delta = H/h_0$)
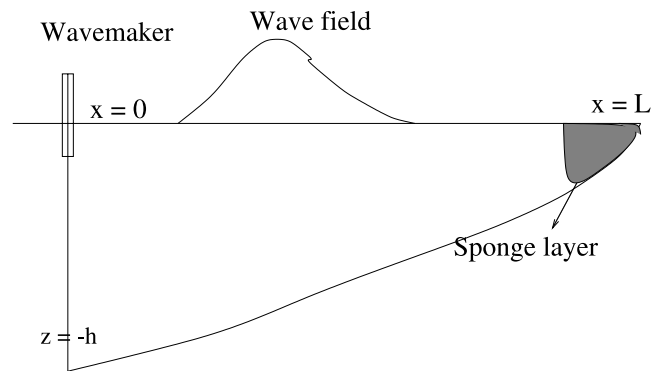
Figure 1. Model domain.

and the relative water depth ($\mu = kh_0$) at the offshore edge of the domain, are 0.16 and 0.24, respectively. Hence they are consistent with the long wave assumptions of the KdV equations. Wave and grid parameters are listed in Table 3.

[43] Waves from a random wave spectrum populate the domain prior to the primary wave spectrum arriving; this is equivalent to the arrival of swell from a distant storm. We run the model using five different initial conditions. Our standard case is a short wave with peak frequency of 1 s^{-1} and maximum wave height of 0.02 m. This corresponds to a relative water depth (μ) of 1.6 and relative wave height (δ) of 0.05. Hence these waves are indeed of a short wavelength. We use the short-wave case for data involving snapshots. A different initial condition is used for the inversion involving time series data. This is a no-wave initial condition ($\delta = 0$). The other initial conditions are discussed in section 5.4. The irregular short waves are run for 24 s each before the long waves are introduced into the domain. The time is initialized from the introduction of the irregular long waves. Hence "early times" and "late times" are with reference to the introduction of irregular long waves.

[44] By performing a least squares minimization, we obtained the results for parameters that best fit the Duck profile for the different parameterizations. Overlaid on the actual Duck bathymetry in Figure 2 are the best fit bathymetries resulting from this parameter search.

[45] We describe the results for the three metrics: column magnitudes of the sensitivity matrix **A**, 2-norm of the columns of **A**, and scaled condition number of **A** in three subsections. For each of the metrics, we introduce the results for data collected as snapshots and time series. Within these results, we describe the results for the different parameterizations. We will also compare results for the different initial conditions for one representative parameterization at the end of the section.

[46] Phase-resolving models such as the KdV model restrict the type of data that may be used for the inversion. When inverting with snapshots, we need two (or more) snapshots and one time series ($\eta(0, t)$) for this type of full inversion approach. In case of periodic or random waves entering the domain, a boundary forcing ($\eta(0, t)$) is essential. This is akin to having access to an offshore wave gauge that collects time series data.

[47] In contrast, when inverting with time series data, we need two (or more) time series and one snapshot ($\eta(x, 0)$) for inversion to be possible. The snapshot serves as the

Table 3. Flow Parameters

Parameter	Symbol	Value
Model Flow Parameters		
Maximum wave height	$\eta_{\max}$	0.065 m
Maximum water depth	h_0	0.4 m
Input wave number	k	0.6 m^{-1}
Length of domain	L	35 m
Equivalent Duck Parameters		
Maximum wave height	$\eta_{\max}$	2.09 m
Maximum water-depth	h_0	12.86 m
Input wave number	k	0.6 m^{-1}
Length of domain	L	1125 m
Computational Grid Parameters		
Time step	Δt	0.01 s
Grid spacing	Δx	0.01 m
Number of points	M	3500
Time period	T	5 s
Nondimensional Parameters		
Relative water depth	kh_0	0.25
Wave steepness	$\eta_{\max}/h_0$	0.16
Ratio of length to depth	L/h_0	87.5

initial condition to the model and is necessary for the phase-resolving type models.

5.1. Column Magnitudes of the Sensitivity Matrix, A

5.1.1. Snapshots

[48] The columns of the sensitivity matrix **A**, for the discrete depth parameters are plotted in Figure 3. There are 100 unknown depth parameters distributed evenly between 0 and 35 m, and there are 3500 surface elevation measure-ment locations, leading to an **A** matrix that is 3500 × 100. A single snapshot at 8 s is used. This corresponds to a nondimensional time t' ($= t/T$) of 1.6. The magnitudes of the elements in two of the 100 columns are shown in Figure 3. We arbitrarily select the 25th parameter ($x = 8.75$ m) and the 40th parameter ($x = 14$ m).

[49] First, if the bathymetry at a location of interest is perturbed, the surface elevation perturbation is a maximum at that location. Second, these surface elevation perturba-tions are nontrivial only in its immediate neighborhood. This indicates that the influence of bathymetry on wave surface elevation is very localized for bathymetry defined by individual discrete depths. Thus a surface measurement at a particular location is sensitive only to bathymetry immediately beneath it (or near by), and individual water depths estimated in this particular manner should either use closely spaced data or rely on interpolation techniques to construct the bathymetry between inversion locations.

[50] In the Bruun/Dean parameterization, the two col-umns of the sensitivity matrix corresponding to the two parameters are plotted in Figure 4 for snapshots at $t' = 1.6$ and 3.2. The x-coordinate is nondimensionalized by the maximum offshore water depth h_0 such that $x' = x/h_0$. Hence x' varies from 0 at the source to 87.5 at the coast. At $t' = 1.6$ (top figure), the wave has propagated up to $x' = 45$. Unlike the discrete depth parameters, influence of Bruun/Dean parameters on sensitivity magnitudes is not localized, meaning that surface elevation measurements over the entire domain ($0-87.5$) are not necessary for estimation of B or β. This tendency makes physical sense, since the Bruun/Dean parameterization defines the entire cross-shore profile rather than a single point in space.
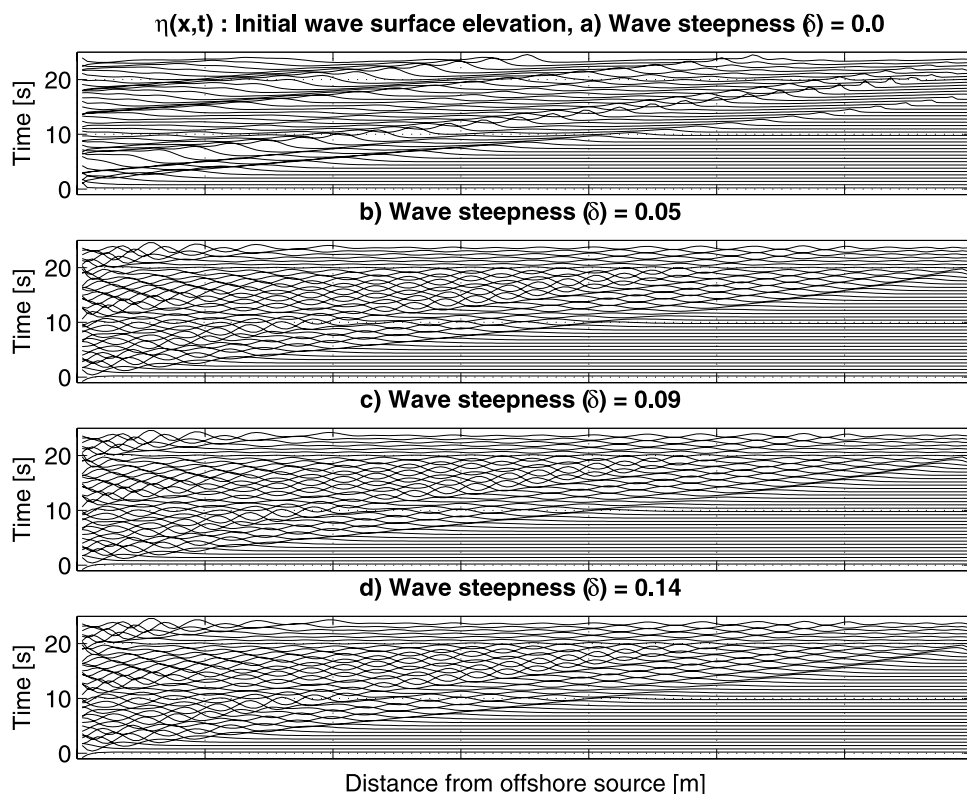
Figure 2. Initial wave surface elevation is plotted for different wave steepnesses.
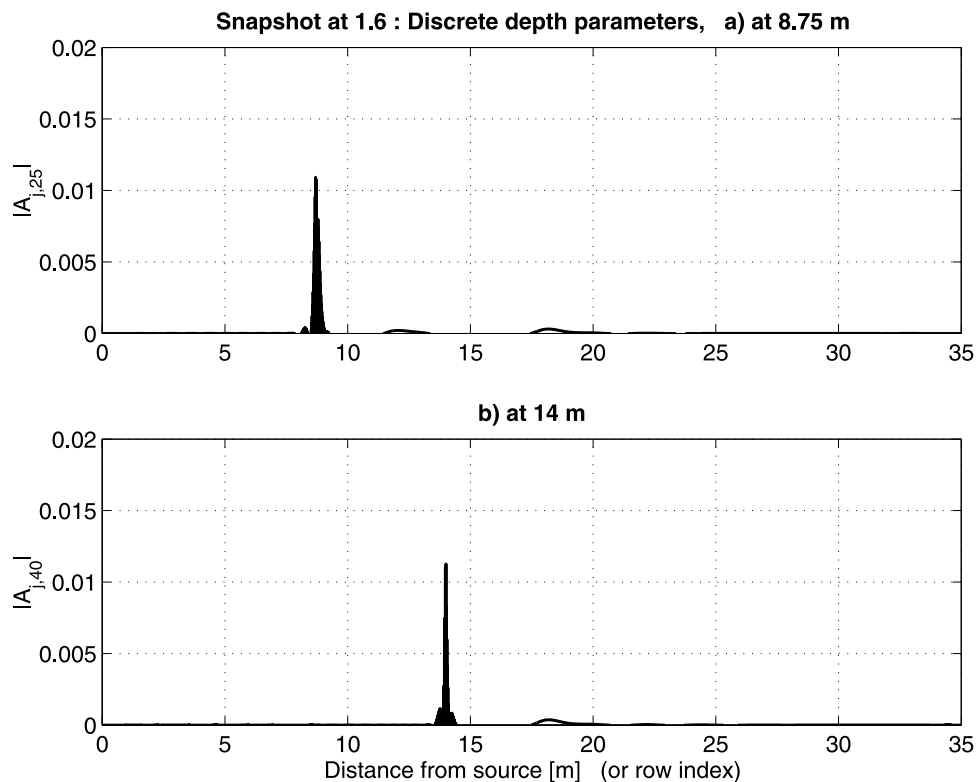
Figure 3. Snapshot data showing magnitude of the columns of the sensitivity matrix, for discrete depth parameters. As noted in the text, the distance from the source to the shore (35 m) is described by 100 discrete depth parameters. The 25th and 40th columns corresponding to depths at 8.75 m and 14 m are plotted for a snapshot at nondimensional time $t' = 1.6$. A change in bathymetry at these locations perturbs the surface elevation only immediately above it.

[51] Further, sensitivity magnitude of B is greater than that of β at all locations, indicating that the former is better constrained by the data. Thus, if data were limited to the offshore side of the domain, B will be better estimated, with lower parameter variance, compared to β. This is logical from a physical point of view; the degree of curvature in the profile is most pronounced nearest the shoreline, and this curvature is dictated by the exponent β. Conversely, the parameter B dictates the profile mean slope; the profile most resembles a linear slope nearest the offshore boundary.

5.1.2. Time Series

[52] The elements of column magnitude of the sensitivity matrix for discrete depth parameterization is plotted in Figure 5 for time series data collected at $t' = 40$. All 100 columns are plotted, and this shows that the maximum sensitivity is at the same location as the time series. Thus, with time series data and discrete depth parameterization, bathymetry is most reliably estimated only immediately beneath the measurement location, a conclusion similar to that with snapshot data.

5.2. The 2-Norm of the Columns of A

[53] The norm of the columns are computed at different times for snapshots and at different locations for time series. The scaled version of this metric is illustrated here.

5.2.1. Snapshots

[54] The norms for Bruun/Dean, Exponential, and Polynomial parameterizations are presented in Figure 6. In the three parameterizations, multiple curves corresponding to the number of unknown parameters are plotted as a function of the snapshot time.

[55] Overall, sensitivity, as quantified by the 2-norm, increases with time for all parameterizations. This is because as time increases, the waves from the source traverse over greater sections of the bathymetry between the source and shore. Hence a snapshot of wave elevation at a later time has more information about the underlying bathymetry, and this is manifest as increased sensitivity. However, sensitivity levels off at or close to $t' = 3.5$, for all parameters. This is the time it takes for the leading wave to propagate from source to the shore, and snapshots at times beyond 3.5 do not provide any new information. Thus snapshots are best acquired at times corresponding to when the leading wave has propagated over most or all of the spatial domain of interest. With real data, there is no concept of a zero time, and with two snapshots, the first is used as an initial condition and the inversion adjusts bathymetry until the predictions match the second snapshot. The above results indicate that the time difference between these two snapshots must be comparable to the time it takes for the waves to reach the shore, to invert for the bathymetry up to the shore.

[56] The 2-norm of different parameters levels off at different times. Consider Bruun/Dean, where it is about $t' = 2.6$ for B while it is $t' = 3.6$ for β. For the former, propagation of the wave in the nearshore does not provide any additional sensitivity.
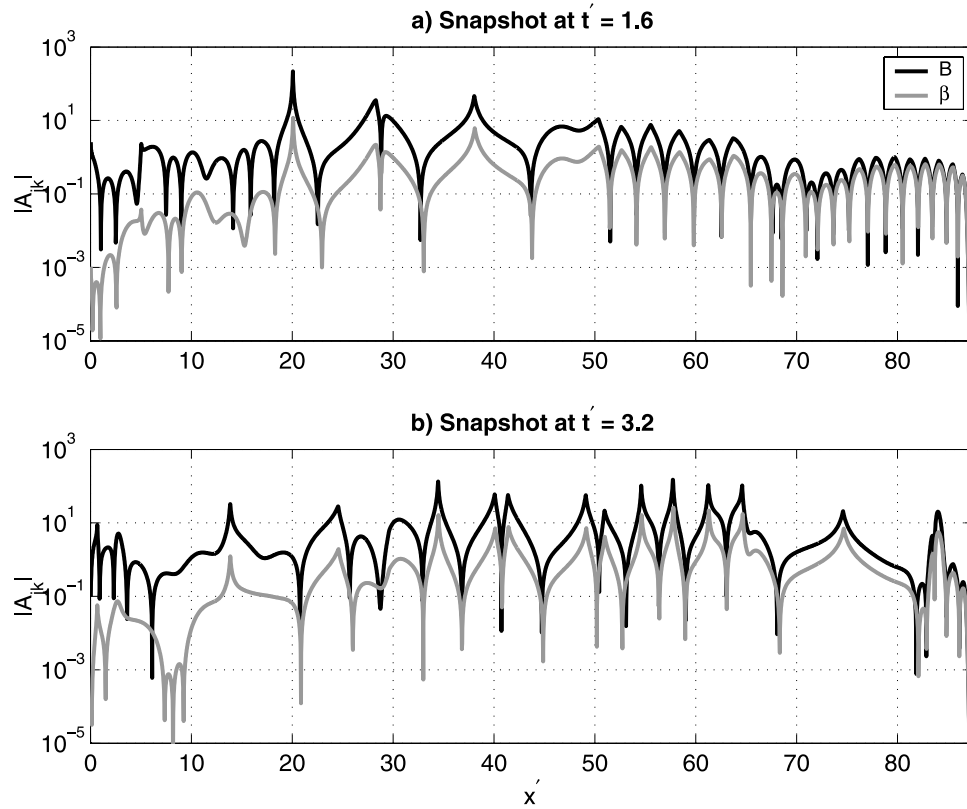
Figure 4. Snapshot data showing magnitude of the columns of the sensitivity matrix, for Bruun/Dean parameterization. Note that the time and distance are represented in the nondimensional form as $t' = t/T$ and $x' = x/h_0$, respectively.
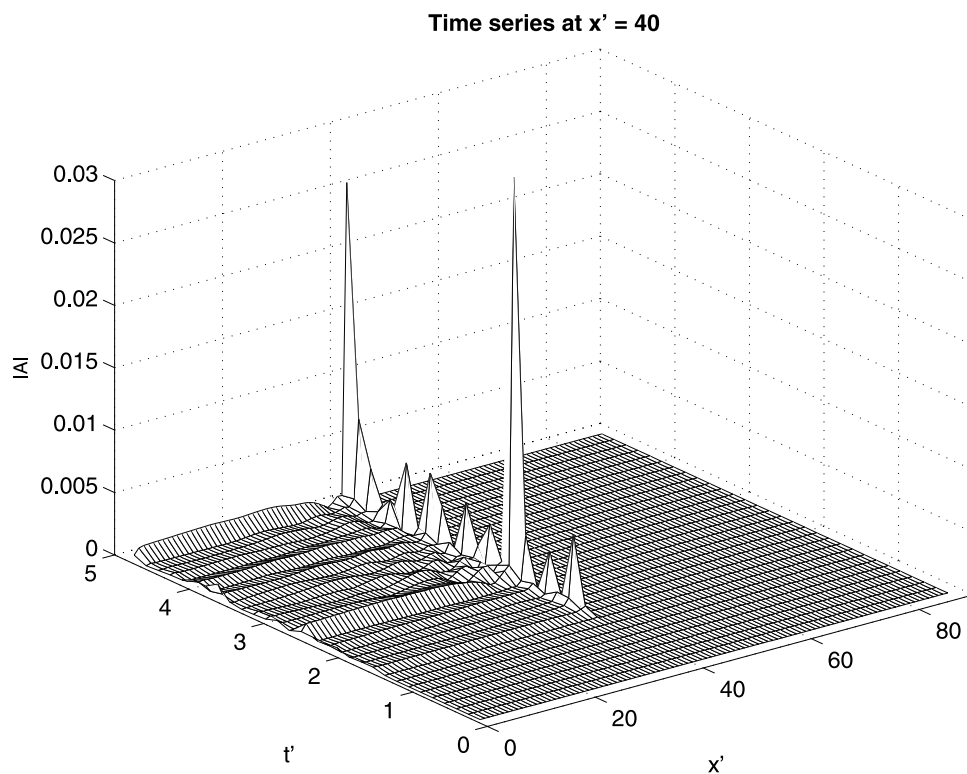
Figure 5. Time series data showing magnitude of the columns of the sensitivity matrix, for discrete depth parameterization. Note that the time and distance are represented in the nondimensional form as $t' = t/T$ and $x' = x/h_0$, respectively.
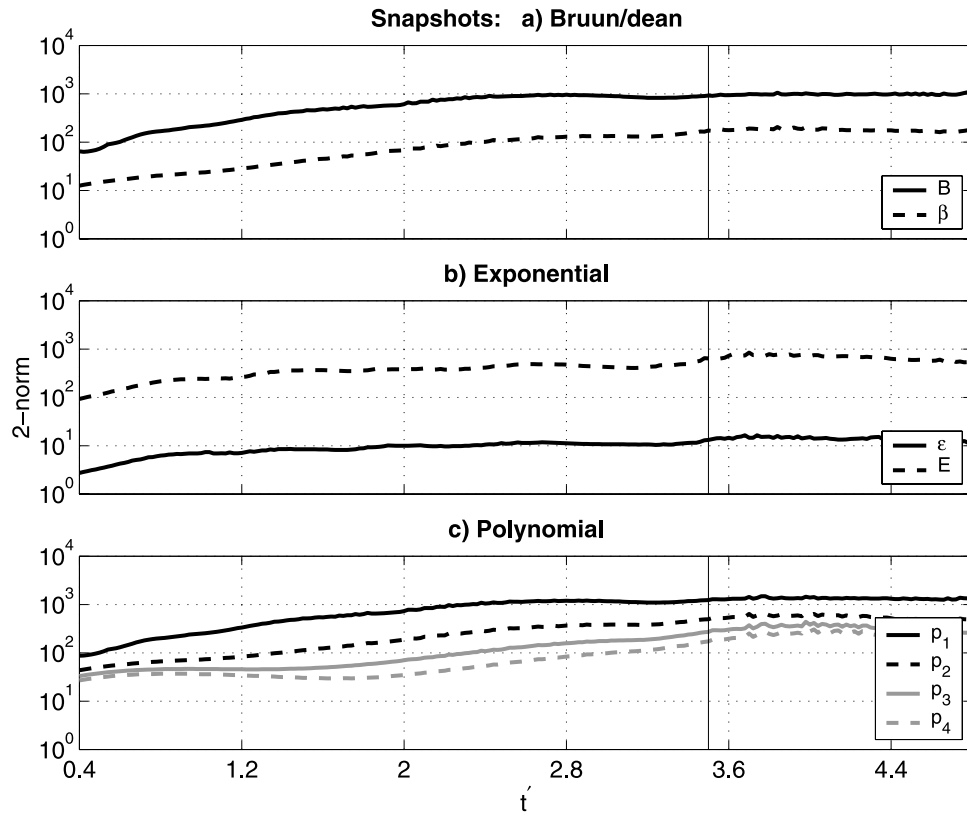
Figure 6. Snapshot data showing 2-norm of the columns of sensitivity matrix, for (a) Bruun/Dean, (b) Exponential, and (c) Polynomial parameterizations. Solid vertical line identifies time when the leading edge of the wave reaches shore. Later times, when the wave is close to the shore, are preferred, as this metric is at/close to its maximum. Note that the time is represented in the nondimensional form as $t' = t/T$.

[57] These differences between parameters can be explored further as follows. The plot of the derivative of bathymetry, h, with respect to parameters of Bruun/Dean, Exponential, and Polynomial profiles is shown in Figure 7. The curves for the Bruun/Dean profile show that influence of B on h is a maximum offshore and it decreases to zero at the shore, while β's influence on h is a maximum close to the shore and decreases in the offshore direction. Therefore changes in B mainly alters the offshore bathymetry, while the nearshore bathymetry (x' is $80-87.5$ from source) is defined by β. This is the reason why the 2-norm levels off at a later time for β compared to B. Therefore, to obtain a good estimate of nearshore bathymetry, β needs to be estimated accurately, which implies that nearshore data is critical (see Figure 6). In the Exponential parameterization, both parameters have the greatest influence on offshore bathymetry, and in the Polynomial parameterization, with the exception of the constant term, the remaining parameters have their greatest influence near the shore.

[58] In Bruun/Dean, the sensitivity of β is less than B at all times. Hence, being a parameter that is better defined by the data, B will converge earlier and would be associated with a smaller parameter variance. Likewise, E will be easier to estimate compared to ϵ in the Exponential model. For the Polynomial, the constant term would be the first to be estimated, with the higher-order terms following in sequence.

5.2.2. Time Series

[59] The 2-norms of $\mathbf{A_s}$ are plotted for the Bruun/Dean and Polynomial parameterizations, in Figure 8. The Exponential model has been omitted since it is qualitatively similar to Bruun/Dean.

[60] The time series at any location incorporates information about the bathymetry between the source and the measurement location. If reflections from the shore can be measured, information about the remaining bathymetry is also present in the time series data. However, in most real situations, including the simulation here, reflections from the shore are negligible. Thus time series need to be collected close to the shore, to be able to invert for bathymetry up to the shore. This is reflected in the Bruun/Dean curves, where sensitivity increases for both parameters as time series are collected closer to the shore. With two measured time series, the offshore measurement is treated as a source and the inversion attempts to match the nearshore measurement by adjusting the bathymetry. On the basis of the above analysis, the latter measurement is best done as close to the shore as possible, to maximize the domain over which bathymetry can be inverted.

[61] Sensitivity of B is greater than that of β and similar to the snapshot case. It is expected that B would converge earlier and would be associated with lesser uncertainty compared to β.
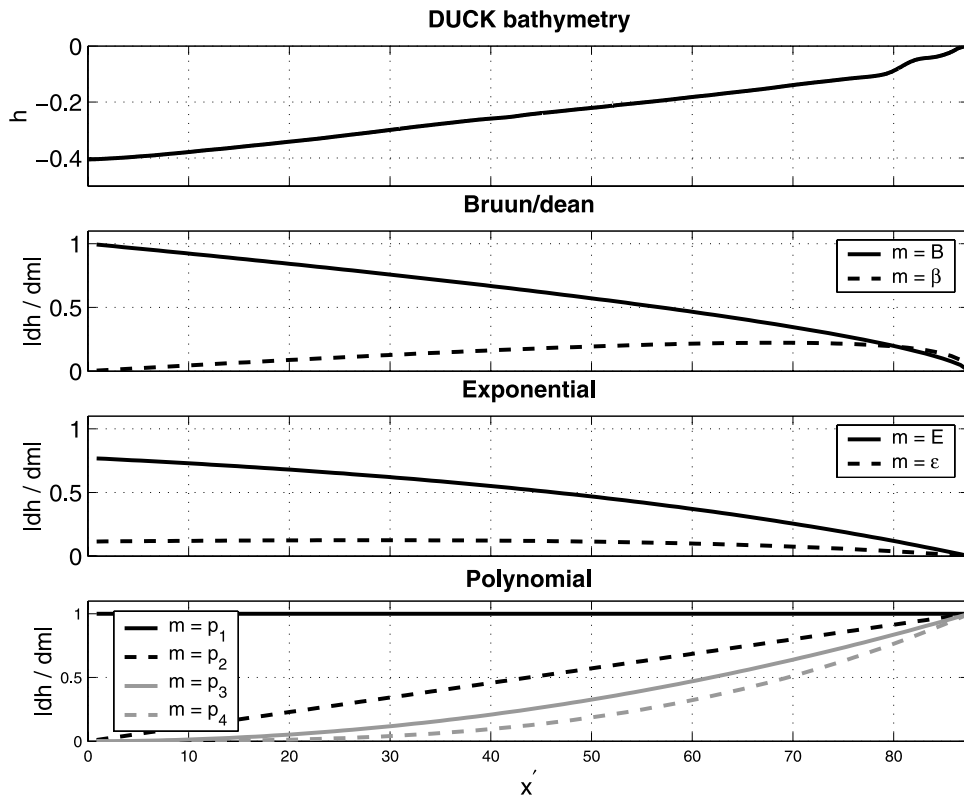
Figure 7. Influence of parameters on bathymetry. Note that the distance is represented in the nondimensional form as $x' = x/h_0$.
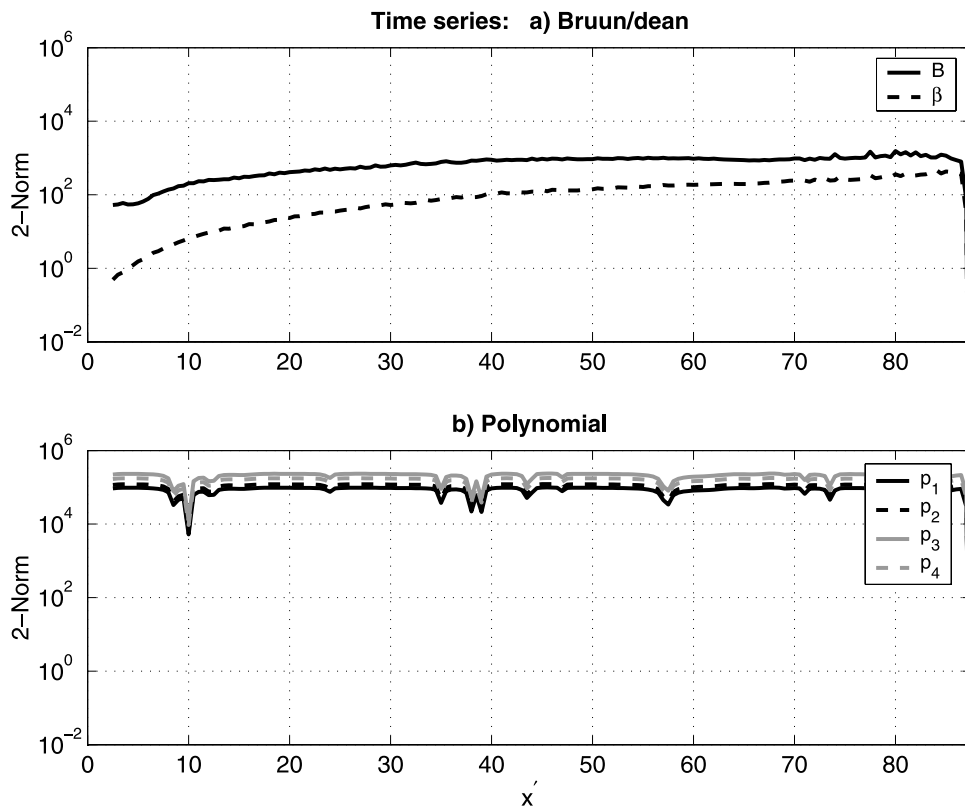
Figure 8. Time series data showing 2-norm of the columns of sensitivity matrix, for (a) Bruun/Dean and (b) Polynomial parameterizations. Note that the distance is represented in the nondimensional form as $x' = x/h_0$.
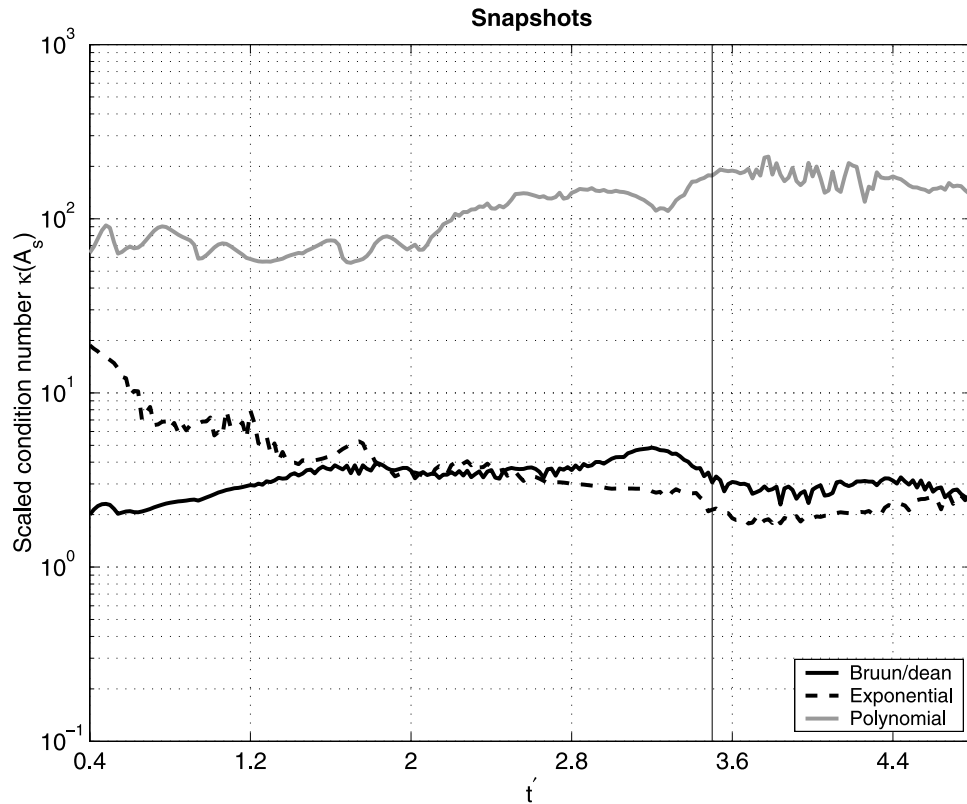
Figure 9. Snapshot data showing scaled condition number $\kappa(\mathbf{A}_s)$, according to which Bruun/Dean is better than Exponential which is better than Polynomial parameterization. Minimum possible (best) value of scaled condition number is 1. The solid vertical line represents the time at which the leading edge of the wave reaches the shore. Note that the time is represented in the nondimensional form as $t' = t/T$.

[62] For the Polynomial, sensitivity of all parameters are comparable and are large. There is no obvious trend with distance in the sensitivity, and the curves suggest that time series at almost any location are associated with sensitivity that is very large relative to unity.

5.3. Scaled Condition Number of $\mathbf{A}_s$

[63] The condition number of the sensitivity matrix is estimated for different times for snapshot data and at different locations for time series data. The scaled version of this metric is illustrated here.

5.3.1. Snapshots

[64] The scaled condition numbers of $\mathbf{A}_s$ corresponding to the three parameterizations are plotted in Figure 9. Ideal parameterizations are those that are well conditioned according to this metric, at times when the wave is close to the shore. This allows for a robust inversion with data that is most informative. From Figure 9, Bruun/Dean and Exponential parameterizations are better conditioned relative to the Polynomial at all times, especially at later times when the leading wave is close to the shore. Bruun/Dean is well conditioned even at early times in contrast with the Exponential. The Polynomial is comparatively poorer, with potential for numerical instability.

[65] An obvious extension to the above analysis is to evaluate variations of the above parameterizations. The scaled condition number for Bruun/Dean and Polynomial parameterizations along with their x-normalized versions

are shown in Figure 10 (see section 2.2). For Bruun/Dean, x-normalizing improves the condition number at early times, whereas, for the Polynomial, x-normalization does not have any impact on its conditioning. It can be easily shown that for the Polynomial, x-normalization only results in scaling the sensitivity matrix and hence does not impact its conditioning. All three metrics are close to their preferred values when time separations between the first and last snapshots are comparable to the time to traverse the snapshot domain for the Bruun/Dean or Exponential parameterizations.

5.3.2. Time Series

[66] The scaled condition numbers corresponding to Bruun/Dean and Polynomial parameterizations for time series are plotted in Figure 11. The Polynomial parameterization, which had favorable 2-norm sensitivity (see Figure 8), has poor conditioning indicated by scaled condition numbers that are very large. This ill conditioning makes it a poor choice with time series data. For example, if nonlinear least squares minimization is used, this would most likely lead to severe numerical problems and divergence. This clearly illustrates the need for interpreting the three metrics collectively.

[67] In contrast, Bruun/Dean parameterization is well conditioned at all spatial locations, indicating that time series measurement locations that span the domain of interest can be inverted with this parameterization. It is worth noting that the scaled condition number for Bruun/
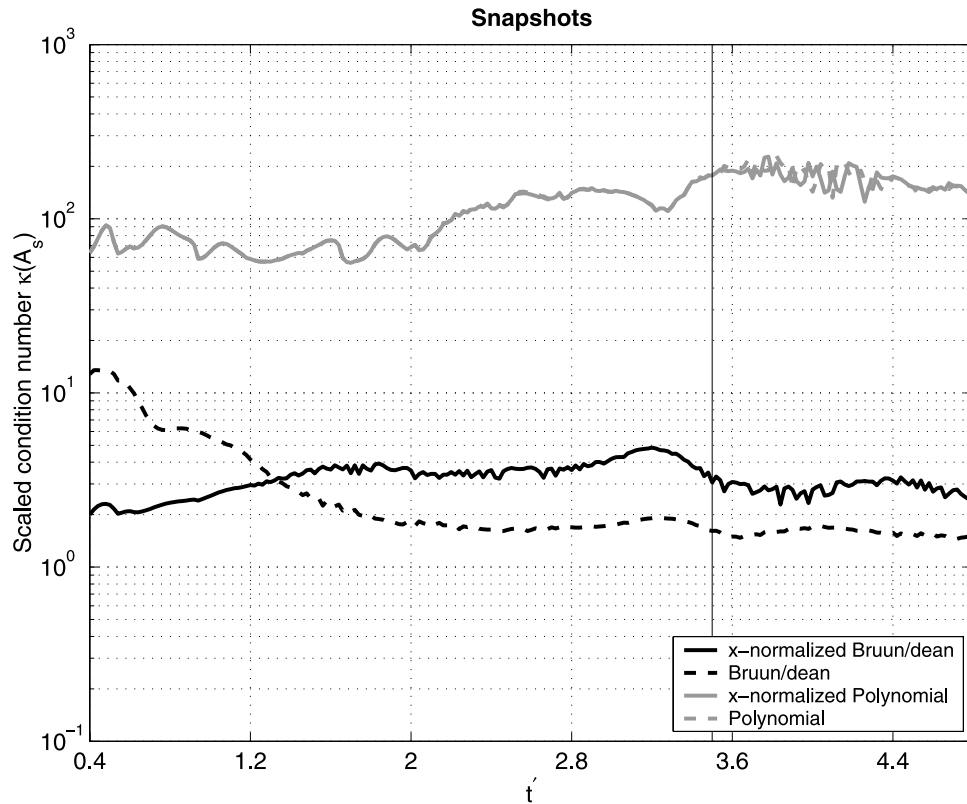
Figure 10. Snapshot data. X-normalizing the Bruun/Dean parameterization improves its conditioning, while it does not have any impact on the Polynomial (both curves coincide). Minimum possible (best) value of scaled condition number is 1. Note that the time is represented in the nondimensional form as $t' = t/T$.

Dean is larger with time series data than snapshots, indicating a preference for the latter type of data.

5.4. Effect of Different Initial Conditions

[68] We evaluate the effect of using different initial conditions on the model sensitivity for the Bruun/Dean parameterization: three short-wave initial conditions, one long-wave, and a no-wave initial condition. We choose the Bruun/Dean parameterization with snapshot data to illustrate this effect.

5.4.1. Short Waves

[69] Waves from a random, high-frequency wave spectrum populate the domain prior to the primary wave spectrum arriving; this is equivalent to the arrival of swell from a distant storm. We run the model using three different initial conditions with δ of 0.05 (standard), 0.1, and 0.15. The peak frequency in all the cases is 1/s, and the model is run for 24 s before the long waves enter the domain.

[70] Figure 12 shows the free wave surface elevation condition for the three different short-wave conditions. In all the three cases, waves are present all over the domain at this time. Since the waves are short, they do not "feel" the bottom. We plot the 2-norm for snapshot data collected at every time (Figure 13). The figure shows that the three initial conditions produce very similar results. Further, we plot the scaled condition number ($\kappa(\mathbf{A_s})$) for all the three cases (see Figure 15 in section 5.4.2). Two other cases are presented that will be discussed in the next sections. All

three cases are very well conditioned. Therefore the results are relatively insensitive to the changes in initial short-wave conditions and have little impact on the sensitivity analysis.

5.4.2. No Waves

[71] For the initial condition with no waves initially in the domain ($\eta(x, 0) = 0.$), the 2-Norm is shown in Figure 14 and the scaled condition number ($\kappa(\mathbf{A_s})$) is shown in Figure 15. The $\delta = 0$ case shows much poorer conditioning compared to the three shortwave conditions.

5.4.3. Long Waves

[72] We ran the model for 100 s and collect the snapshot at that time. We use this as the initial condition for the model. Spectrally, the initial condition is now similar to the incoming waves. We perform the same analysis and plot the 2-Norm and scaled condition number in Figures 14 and 15. Again, the sensitivity results show very similar behavior to the case of no waves and short waves.

[73] The initial conditions have very little effect on the sensitivity analysis. Hence the sensitivity analysis can be conducted with the simplest initial condition: no waves inside the domain.

6. Conclusion

[74] We present a general method for approaching full inversion of bathymetry parameters from surface wave data. Before a computationally intensive full inversion is conducted, it is important that the appropriate data and model
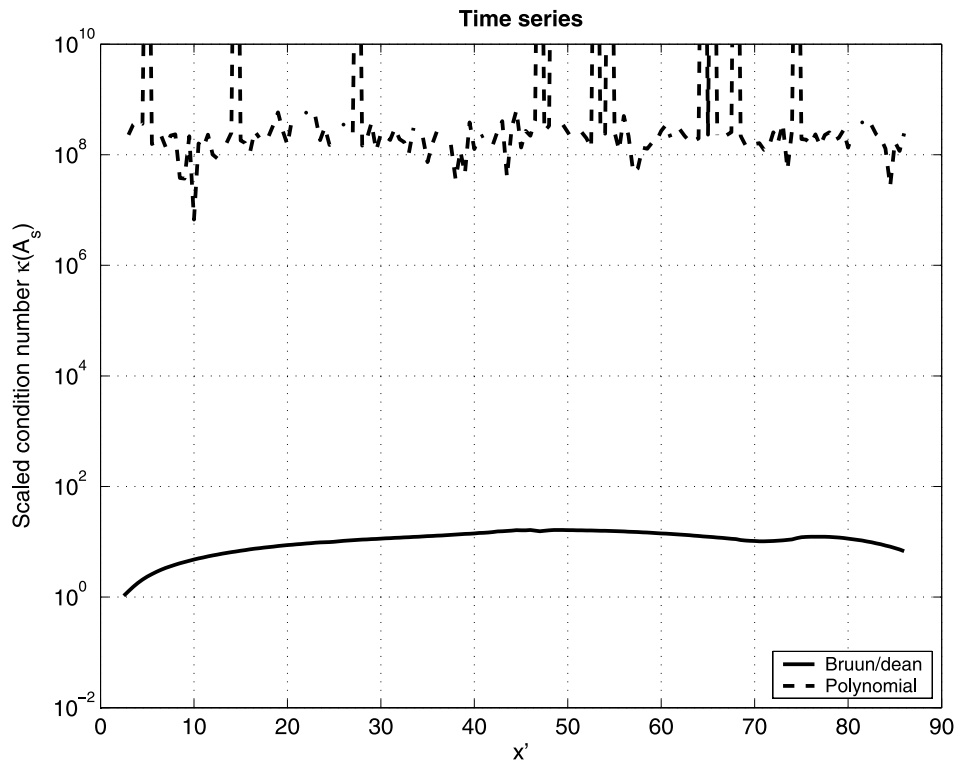
Figure 11. Time series data showing scaled condition number $\kappa(\mathbf{A}_s)$, according to which Bruun/Dean parameterization can be used with time series data, while the Polynomial parameterization will likely be associated with numerical instability. Note that the distance is represented in the nondimensional form as $x' = x/h_0$.
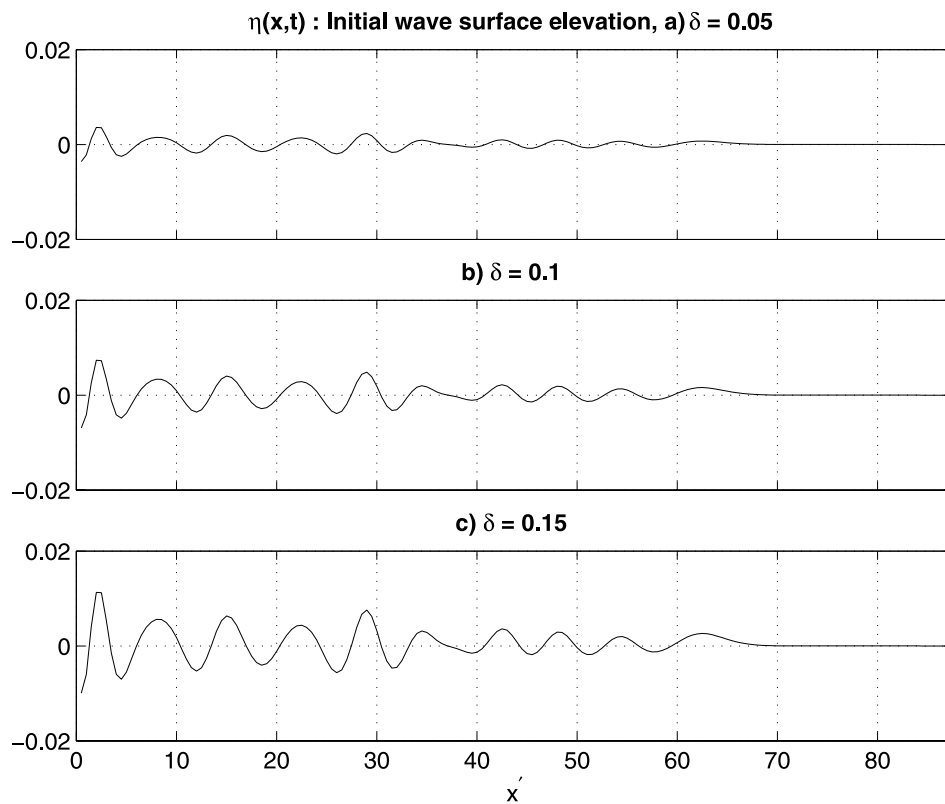
Figure 12. Free wave surface elevation condition for the three different short wave conditions: $\delta = 0.05$ (standard), 0.1, and 0.15 at $t = 24$ s is shown. Note that this represents the initial condition before the long waves are introduced. Note that the distance is represented in the nondimensional form as $x' = x/h_0$.
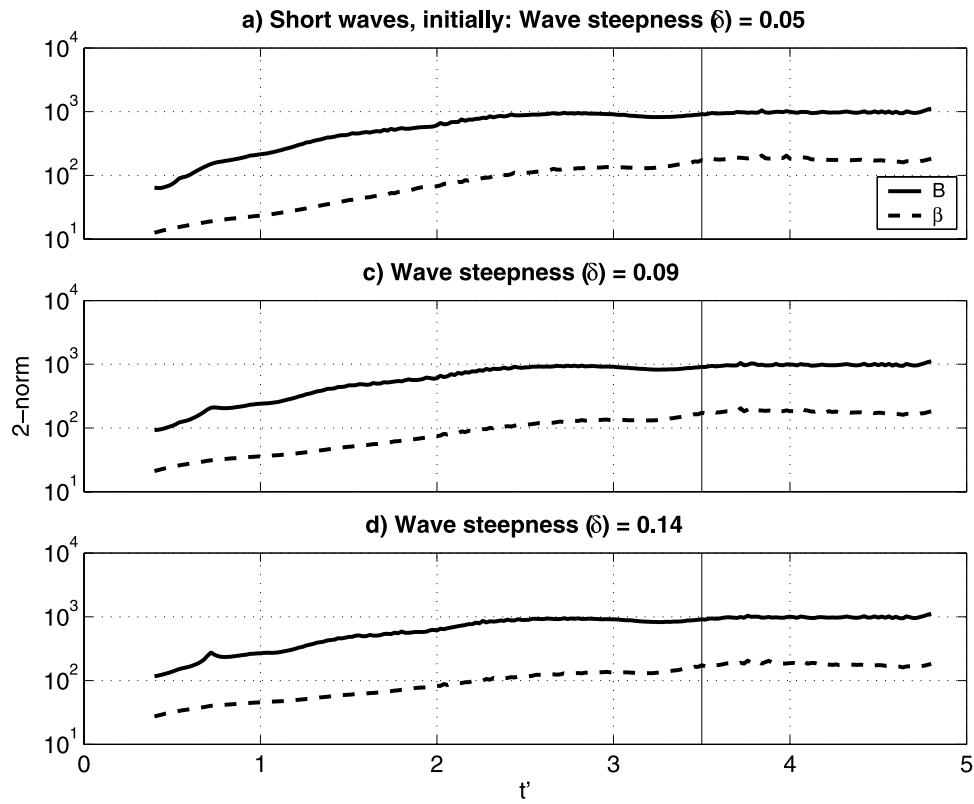
Figure 13. Snapshot data showing the 2-norm of the columns of sensitivity matrix, for Bruun/Dean parameterization for the three short wave δ cases: 0.05, 0.1, and 0.15. All three cases show similar results. Note that the time is represented in the nondimensional form as $t' = t/T$.
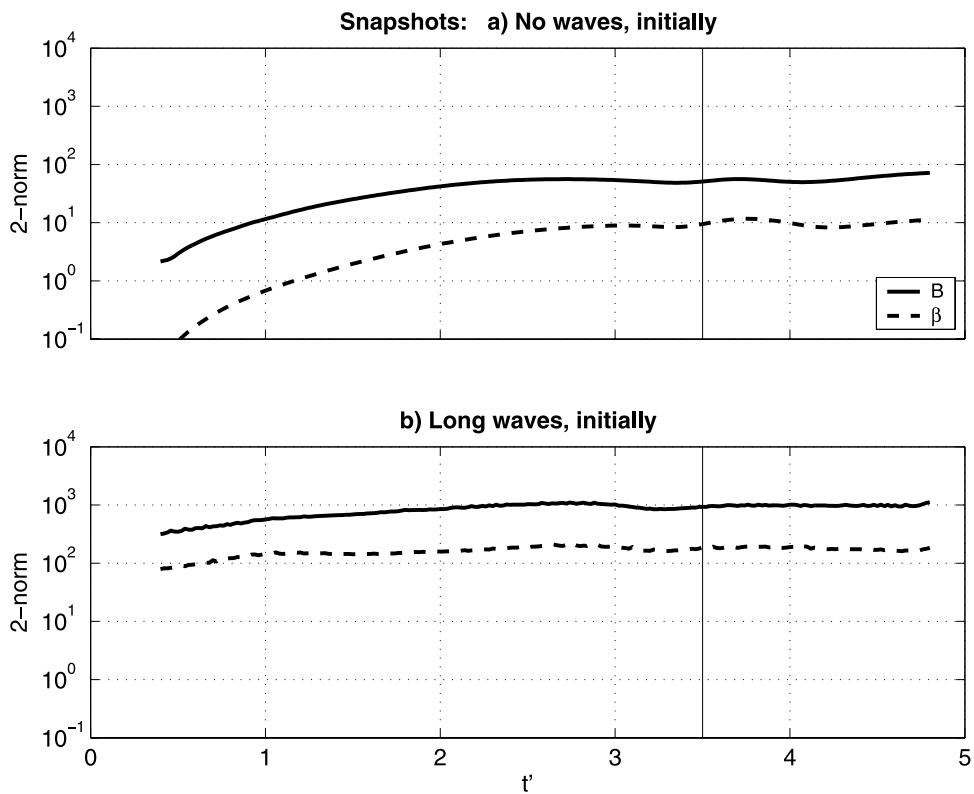
Figure 14. Snapshot data showing the 2-norm of the columns of sensitivity matrix, for Bruun/Dean parameterization for the no-waves and long-waves cases are shown. Note that the time is represented in the nondimensional form as $t' = t/T$.

Snapshots: Bruun/Dean paramterization for different wave steepness
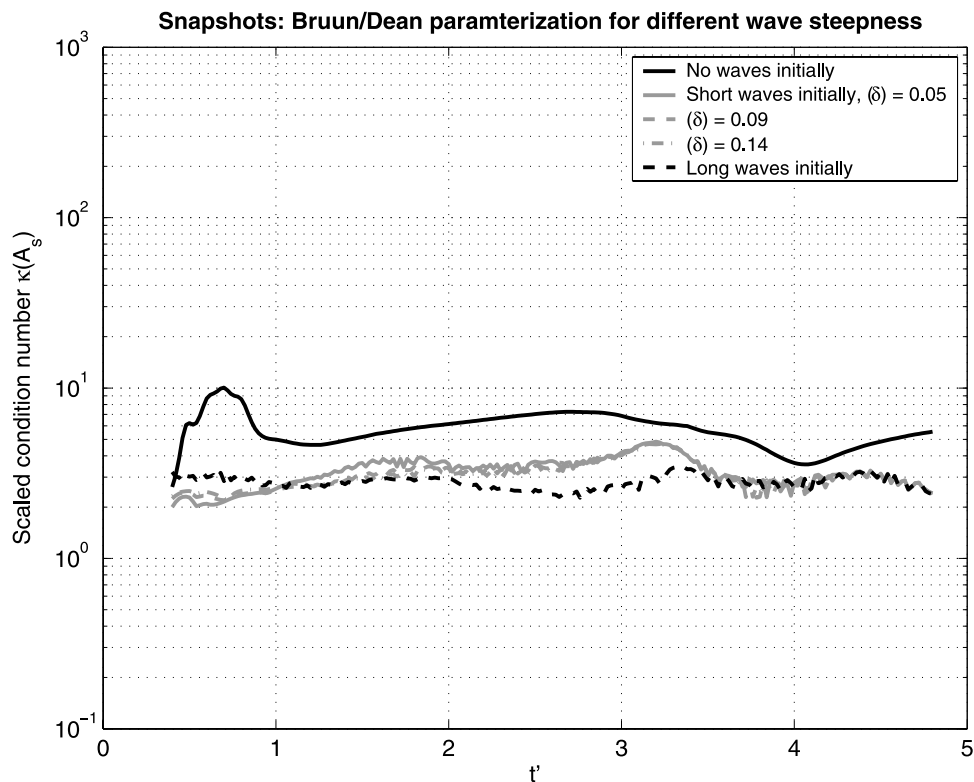
Figure 15. Snapshot data. Scaled condition number $\kappa(\mathbf{A}_s)$ for all five different initial conditions using the Bruun/Dean parameterization case is shown. Minimum possible (best) value of scaled condition number is 1. Note that the time is represented in the nondimensional form as $t' = t/T$.

structure be selected in a manner that mitigates complications related to parameter identifiability and yields robust bathymetry estimates.

[75] We illustrate how guidelines for experiment design and bathymetry parameterization can be derived by minimizing the parameter variances. The results indicate that the choices for both are interlinked; that is, the available data guides the parameterizations that can be used or the chosen parameterization (depending on the a priori bathymetry information) drives data acquisition choices. This analysis is independent of the inversion technique itself and would be performed before the performing the inversion.

6.1. Model Parameterization

[76] Among the parameterizations investigated here, Bruun/Dean and Exponential bathymetric parameterizations are the most conducive for inversion with both time series and snapshot data. Bathymetric inversion using Polynomial representation may work with snapshot data, while it will likely encounter severe numerical difficulties with time series data.

[77] The choice of bathymetry parameterization impacts the success of inversion and is to be driven by valid prior knowledge. Arbitrary parameterizations may not necessarily be well conditioned, while very general parameterizations like discrete water depths introduce large numbers of unknown parameters. Further, assumed parameterizations allow for estimation of bathymetry outside the domain of observation, but whose estimates are only as good as the underlying assumption. For example, with

Bruun/Dean or Exponential type bathymetry assumption, snapshot observations over which waves have not reached the shore may allow the estimation of bathymetry up to the shore. In contrast, with discrete depths, an arbitrary bathymetry can be reliably inverted, but only within the domain of observations.

6.2. Experimental Design

[78] Ideally, data of two or more snapshots are acquired so that the time separation between the first and last snapshot is comparable to the time it takes for waves to traverse the measurement domain. Similarly, with two or more time series, the spatial range of the measurements spans the domain of interest. If Polynomial parameterization is chosen, nearshore snapshot data are critical for reliable estimation of bathymetry up to the shore, whereas with Bruun/Dean and Exponential parameterizations the same may be accomplished with snapshot or time series data that are acquired farther offshore.

References

Beck, M. B. (1987), Water quality modeling: A review of the analysis of uncertainty, *Water Resour. Res.*, *23*(8), 1393–1442.

Bell, P. S. (1999), Shallow water bathymetry derived from an analysis of X-band marine radar images of waves, *Coastal Eng.*, *37*, 513–527.

Belsley, D. A. (1991), *Conditioning Diagnostics*, 396 pp., John Wiley, New York.

Bennett, A. F. (1992), *Inverse Methods in Physical Oceanography*, 346 pp., Cambridge Univ. Press, New York.

Birkemeier, W. A., C. Donoghue, C. E. Long, K. K. Hathaway, and C. F. Baron (1997), 1990 DELILAH nearshore experiment: Summary report, *Tech. Rep. CHL-97-24*, U.S. Army Corps of Eng., Washington, D. C.

Bodge, K. R. (1992), Representing equilibrium beach profiles with an Exponential function, *J. Coastal Res.*, 8, 47–55.

Bona, J. L., and P. J. Bryant (1973), A mathematical model for long waves generated by wave makers in nonlinear dispersive systems, *Proc. Cambridge Philos. Soc.*, 73, 391–405.

Brun, R., P. Reichert, and H. R. Kunsch (2001), Practical identifiability analysis of large environmental simulation models, *Water Resour. Res.*, 37(4), 1015–1030.

Bruun, P. (1954), Coastal erosion and the development of beach profiles, *Tech. Memo. 44*, 79 pp., Beach Erosion Board, U.S. Army Corps of Eng., Washington, D. C.

Chavent, G. (1987), Identifiability of parameters in the output least square formulation, in *Identifiability of Parameteric Models*, edited by E. Walter, Pergamon, New York.

Chen, Q., J. T. Kirby, R. A. Dalrymple, A. B. Kennedy, and M. C. Haller (1999), Boussinesq modeling of a rip current system, *J. Geophys. Res.*, 104, 20,617–20,637.

Chen, Q., J. T. Kirby, R. A. Dalrymple, A. B. Kennedy, and A. Chawla (2000), Boussinesq modeling of wave transformation, breaking and runup: II. Two horizontal dimensions, *J. Waterw. Port Coastal Ocean Eng.*, 126, 48–56.

Dean, R. G. (1977), Equilibrium beach profiles: U.S Atlantic and Gulf coasts, *Ocean Eng. Tech. Rep. 12*, Dep. of Civ. Eng., Univ. of Dela., Newark.

Dean, R. G. and R. A. Dalrymple (2001), *Coastal Processes with Engineering Applications*, 488 pp., Cambridge Univ. Press, New York.

de las Heras, M. M., and P. A. E. M. Janssen (1992), Data assimilation with a coupled wind-wave model, *J. Geophys. Res.*, 97, 20,261–20,270.

Dugan, J. P., H. H. Suzukawa, C. P. Forsyth, and M. S. Farber (1996), Ocean wave dispersion surface measured with airborne IR imaging system, *IEEE Trans. Geosci. Remote Sens.*, 34(5), 1282–1284.

Eilbeck, J. C., and G. R. McGuire (1975), Numerical study of the regularized long wave equation: 1. Numerical methods, *J. Comput. Phys.*, 19, 43–57.

Feddersen, F., R. T. Guza, and S. Elgar (2004), Inverse Modeling of the one-dimensional setup and alongshore current in the nearshore, *J. Phys. Oceanogr.*, 324, 920–933.

Ghil, M. (1989), Meteorological data assimilation for oceanographers: I. Description and theoretical framework, *Dyn. Atmos. Oceans*, 13, 171–218.

Grilli, S. T. (1998), Depth inversion in shallow water based on nonlinear properties of shoaling periodic waves, *J. Coastal Eng.*, 35, 185–209.

Hayden, B., W. Felder, J. Fisher, D. Resio, L. Vincent, and R. Dolan (1975), Systematic variations in inshore bathymetry, *Tech. Rep. 10*, Dep. of Environ. Sci., Univ. of Va., Charlottesville.

Holland, K. T. (2001), Application of the linear dispersion relation with respect to depth inversion and remotely sensed imagery, *IEEE Trans. Geosci. Remote Sens.*, 39(9), 2060–2072.

Hughes, S. A. (1984), TMA shallow-water spectrum: Description and application, *Tech. Rep. CERC-84-7*, U.S. Army Eng. Waterw. Exper. Stn., Vicksburg, Miss.

Hwang, P. A., W. Wright, W. B. Krabill, and R. N. Swift (2001), Airborne remote sensing of breaking waves, *Remote Sens. Environ.*, 78, 1–11.

Kaihatu, J. and C. Narayanan (2001), Refinements to an optimized model-driven bathymetry deduction algorithm, paper presented at Waves 2001 Conference, Am. Soc. of Civ. Eng., San Fransisco, Calif.

Kennedy, A. B., R. A. Dalrymple, J. T. Kirby, and Q. Chen (2000), Determination of inverse depths using direct Boussinesq modeling, *J. Waterw. Port Coastal Ocean Eng.*, 126, 206–214.

Kitamura, S., and S. Nakirigi (1977), Identifiability of spatially-varying and constant parameters in distributed systems of parabolic type, *SIAM J. Control Optim.*, 15, 785–802.

Kokotovich, P. (1964), Method of sensitivity points in the investigation and optimization of linear control systems, *Autom. Remote Control*, 25, 1512–1518.

Komar, P. D., and W. G. McDougal (1994), The analysis of Exponential beach profiles, *J. Coastal Res.*, 10, 59–69.

Kreindler, E. (1968), On the definition and application of the sensitivity function, *J. Franklin Inst.*, 285(1), 26–36.

Larson, M. (1995), Model for decay of random waves in the surf zone, *J. Waterw. Port Coastal Ocean Eng.*, 121, 1–12.

Misra, S., A. B. Kennedy, J. T. Kirby, and R. A. Dalrymple (2000), Determining water depth from surface images using Boussinesq equations, paper presented at 27th International Conference on Coastal Engineering, Am. Soc. of Civ. Eng., Sydney, Australia.

Moore, A. M. (1991), Data assimilation in a quasi-geostrophic open ocean model of the Gulf Stream region using the adjoint method, *J. Phys. Oceanogr.*, 21, 398–427.

Narayanan, C., and J. Kaihatu (2000), Use of phase-resolving wave models in bathymetric deduction, paper preseented at 27th International Conference Coastal Engineering 2000, Am. Soc. of Civ. Eng., Sydney, Australia.

Navon, I. M. (1997), Practical and theoretical aspects of adjoint parameter estimation and identifiability in meteorology and oceanography, *Dyn. Atmos. Oceans*, 27, 55–79.

Noble, B. (1969), *Applied Linear Algebra*, Prentice-Hall, Old Tappan, N. J.

Özkan-Haller, H. T., and J. Long (2002), The determination of bottom friction using data assimilation methods, *Eos Trans. AGU*, 83(47), Fall Meet. Suppl., Abstract OS71A-0258.

Press, W. H., B. P. Flannery, S. A. Teukolsky, and W. T. Vetterling (1986), *Numerical Recipes: The Art of Scientific Computing*, pp. 523–538, Cambridge Univ. Press, New York.

Pruszak, Z., and G. Różyński (1997), Variability of multi-bar profiles in terms of random sine functions, *J. Waterw. Port Coastal Ocean Eng.*, 124, 48–56.

Rao, V. N. R. (1996), The radiation and vibration of drilling tubulars in fluid-filled boreholes, Ph.D. thesis, MIT Press, Cambridge, Mass.

Shapiro, R. (1970), Smoothing, filtering and boundary effects, *Rev. Geophys.*, 8, 359–387.

Stockdon, H. F., and R. A. Holman (2000), Estimation of wave phase speed and nearshore bathymetry from video imagery, *J. Geophys. Res.*, 105, 22,015–22,033.

Strang, G. (1980), *Linear Algebra and its Applications*, Academic, San Diego, Calif.

Sun, N., N. Z. Sun, M. Elimelech, and N. R. Ryan (2001), Sensitivity analysis and parameter identifiability for colloid transport in geochemically heterogeneous porous media, *Water Resour. Res.*, 37(2), 209–222.

Thacker, W. C., and R. B. Long (1988), Fitting dynamics to data, *J. Geophys. Res.*, 93, 1227–1240.

Wei, G., J. T. Kirby, S. T. Grilli, and R. Subramanya (1996), A fully nonlinear Boussinesq model for surface waves: 1. Highly nonlinear unsteady waves, *J. Fluid Mech.*, 294, 71–92.

Xia, J., R. D. Miller, and C. B. Park (1999), Estimation of near-surface shear velocity by inversion of Rayleigh waves, *Geophysics*, 64(3), 691–700.

Yu, L., and J. J. O'Brien (1992), On the initial condition in parameter estimation, *J. Phys. Oceanogr.*, 22, 1361–1364.

————————

J. M. Kaihatu, Oceanography Division, Naval Research Laboratory, Code 7322, Stennis Space Center, MS 39529, USA. (kaihatu@nrlssc.navy.mil)

C. Narayanan, Marine Modeling and Analysis Branch, 5200 Auth Road Room 209, Camp Springs, MD 20746, USA. (chandrasekher.narayanan@noaa.gov)

V. N. Rama Rao, Earth Resources Laboratory, Massachusetts Institute of Technology, Cambridge, MA 02142, USA. (rrao@mit.edu)